T.M. Inerbaev[1], Zh.Ye. Zakiyeva[2*], F.U. Abuova[3], A.U. Abuova[4], S.A. Nurkenov[5], G.A. Kaptagay[6]

[1,2,3,4,5] L.N. Gumilyov Eurasian National University, Astana, Kazakhstan;
[5] Astana International University, Astana, Kazakhstan;
[6] Kazakh National Women's Teacher Training University, Almaty, Kazakhstan
([*]E-mail for contacts: zhadyrazakiyeva@gmail.com)

DFT studies of BaTiO3

The structure of stable phases is investigated using first-principle calculations based on the functionals: LDA, GGA and newly developed general-purpose heavily constrained and appropriately normalized meta-GGA-functional (SCAN). The purpose of this study is to theoretically study the atomic displacements and band gap of the cubic, tetragonal, orthorhombic, rhombohedral perovskite phases for the comparison LDA, GGA-PBE and meta-GGA functionals using the density functional theory method. The obtained data of the density of states (DOS) showed that the values of the band gap energies are underestimated, and the DOS values show that the upper part (valence band) mainly consists of O $2p$ orbitals, the lower part (conduction band) consists of Ti $3d$ orbitals. The rhombohedral phase has a mixed composition of Ti states in the conduction band with a greater degree of $3d_{z2}$ than $3d_{xy}$. The values of the energies of the band gap (E_{gap}) and the density of states show reasonable agreement with experimental and theoretical data. The LDA functional and, to a lesser extent, the GGA - PBE functional can also provide fairly accurate information about atomic displacements in these crystals. The values calculated by the SCAN functional do not differ much from the GGA and LDA functionals.

Keywords: perovskite, unit cell, density of states, distortion of atoms, band gap, first-principle calculations, density functional theory, plane waves, space group.

Introduction

Barium titanate - perovskite was discovered half a century ago, but due to its unique crystal structures, physical and chemical properties, the material still attracts a lot of attention of researchers. In addition, barium titanate has a high dielectric constant, and their excellent piezoelectric and ferroelectric properties are also known. Over the past decade, it has become one of the important materials with excellent dielectric, ferroelectric and piezoelectric properties, due to which this type of material has great capabilities, which allows them to be used in the production of electronic devices. It is one of the most thoroughly studied cubic perovskites, and has paraelectric properties at high temperatures and has a simple cubic perovskite structure. Most of the ABO_3 type perovskites have the same stable phases at different temperatures.

Perovskites are complex oxides, mainly of the composition ABO_3, where A is a divalent metal, and B is a tetravalent (transition) metal. Perovskite is the object of scientific research in connection with promising electrical, magnetic, photoelectric and redox properties [1-4] for energy production (SOFC – solid oxide fuel cell technology) [5]. Perovskites can exist in various phace modifications, which generally exhibit different properties. The number of phase modifications depends on the specific combination of A and B cations [1, 6]. Many perovskites, specifically, demonstrate the presence of other phases. The highly symmetrical cubic phase of the *Pm-3m* crystal is also stable at high temperatures and demonstrates a series of three phase transitions with decreasing temperature: tetragonal *I4/mcm* at 393 K, orthorhombic *Amm2* at 278 K and rhombohedral *R3m* at 183 K, as shown in Figure 1.

Over the past 20 years, several first principles calculations have been carried out, in which more attention was paid to the structural and electronic properties of the four phases [7-10]. The theoretical study of this perovskite still requires detailed analysis, since it does not show the same result compared to experimental data and still remains an object research. Experimental data [11] showed band gap widths of about 3.7 eV for the cubic phase and 3.9 eV for the tetragonal phase. In general, density functional theory (DFT) will be applied with a combination of different approximations to describe the structure of the perovskite band gap. The method is distinguished for describing the wave function and allows us to determine the energy state of the system, which includes the stationary Schrodinger equation. In this paper, the width of the forbidden zone with three different functionals is calculated: LDA, GGA and meta-GGA.

Since phases other than the cubic phase have an internal degree of freedom, some of them must be optimized. Thus, DFT calculations are carried out with high accuracy to precisely obtain ferroelectric phases. Minimization is not required for a cubic structure. The tetragonal structure was optimized by changing the coordinates of the ions, since the symmetry (distortion in the z direction) allows optimization in a fixed c/a ratio, while maintaining a fixed volume. Then, using the optimized coordinates of the ion particles, the relation (maybe the ratio) $\frac{c}{a}$ was optimized at a constant volume. Thus, the relation $Ti\left(1/2, 1/2, 1/2 + \Delta z_{Ti}\right)$, $O_1\left(1/2, 1/2, \Delta z_{O_1}\right)$, $O_2\left(1/2, 0, 1/2 + \Delta z_{O_2}\right)$ it has been optimized while minimizing. The lattice parameters were also optimized in the orthorhombic phase: a, b, c and $Ti\left(1/2, 0, 1/2 + \Delta z_{Ti}\right)$ $O1\left(0, 0, 1/2 + \Delta z_{O1}\right)$ $O2\left(1/2, 1/4 + \Delta y_{O2}, 1/4 + \Delta z_{O2}\right)$. Lattice parameter a $\left(a = b = c\right)$, angle α $\left(\alpha = \beta = \gamma\right) \Delta$ $Ti\left(1/2 + \Delta x, 1/2 + \Delta x_{Ti}, 1/2 + \Delta x_{Ti}\right)$ $O\left(1/2 + \Delta x_O, 1/2 + \Delta x_O, 0 + \Delta z_O\right)$ were optimized values for the rhombohedral phase. The atomic positions are shown in Table 1.

Calculation methods

Calculations of the electronic structure were carried out by the density functional method in the basis of plane waves, as implemented in the VASP program code [12, 13]. The method of projection attached waves (projector augmented wave – PAW) was used [14]. LDA [15, 16], GGA with PBE [17], and SCAN [18] meta GGA [19, 20] were used for comparative analysis. The cutting energy of plane waves in all calculations was 520 eV. The partition of the inverse space was chosen using the Monhorst–Pack scheme in the form of an 8×6×6 grid for the orthorhombic phase, 8×8×8 for the tetragonal and rhombohedral phase. Levels were considered as valence states.

Results and discussion

The coordinates of the location of the atoms of the unit cell *BaTiO3*, tetragonal, orthorhombic, and rhombohedral, cubic phase are given in Table 1.

T a b l e 1

Coordinates of the arrangement of atoms in the unit cell $BaTiO_3$.

Cubic phase (Pm3m) SG-221	Tetragonal phase (P4/mmm) SG-99	Orthorhombic phase (Amm2) SG-38	Rhombohedral phase (R3m) SG-160	Ref.
Ba:1a (0,0,0)	Ba:1a(0,0,0)	Ba: 2a (0,0,0)	Ba:1a (0,0,0)	[8]
$Ti : 1b\left(1/2; 1/2; 1/2\right)$	$Ti : 1b\left(1/2, 1/2, 1/2 + \Delta z_{Ti}\right)$	$Ti : 2b\left(1/2, 0, 1/2 + \Delta z_{Ti}\right)$	$Ti : 1a\left(1/2 + \Delta x, 1/2 + \Delta x_{Ti}, 1/2 + \Delta x_{Ti}\right)$	[8]
$O : 3c\left(1/2; 1/2; 0\right)$	$O_1 : 1b\left(1/2, 1/2, \Delta z_{O_1}\right)$	$O1 : 2a\left(0, 0, 1/2 + \Delta z_{O1}\right)$	$O : 3b\left(1/2 + \Delta x_O, 1/2 + \Delta x_O, 0 + \Delta z_O\right)$	[8]
—	$O_2 : 2c\left(1/2, 0, 1/2 + \Delta z_{O_2}\right)$	$O2 : 4e\left(1/2, 1/4 + \Delta y_{O2}, 1/4 + \Delta z_{O2}\right)$	—	[8]

The atom Ba is located in the position (0,0,0), $Ti\left(1/2, 1/2, 1/2 + \Delta z_{Ti}\right)$ and $O_2\left(1/2, 0, 1/2 + \Delta z_{O_2}\right)$ are distortions of Ti and O atoms in a tetragonal structure. In an orthorhombic structure $Ti\left(1/2, 0, 1/2 + \Delta z_{Ti}\right)$ $O1\left(0, 0, 1/2 + \Delta z_{O1}\right)$ and $O2\left(1/2, 1/4 + \Delta y_{O2}, 1/4 + \Delta z_{O2}\right)$ are distortions of Ti and O atoms. In a rhombohedral structure $Ti\left(1/2 + \Delta x, 1/2 + \Delta x_{Ti}, 1/2 + \Delta x_{Ti}\right)$ and $O\left(1/2 + \Delta x_O, 1/2 + \Delta x_O, \Delta z_O\right)$ are distortions of Ti and O atoms [8].
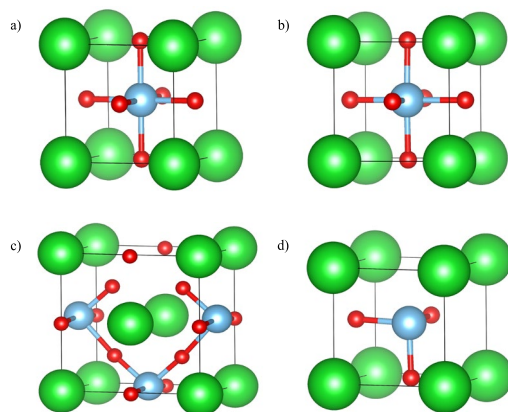
Figure 1. Unit cells *BaTiO3* in cubic, tetragonal, orthorhombic and rhombohedral phases

T a b l e 2

Calculated volumetric properties of the unit cell *BaTiO₃* tetragonal, orthorhombic and rhombohedral phases

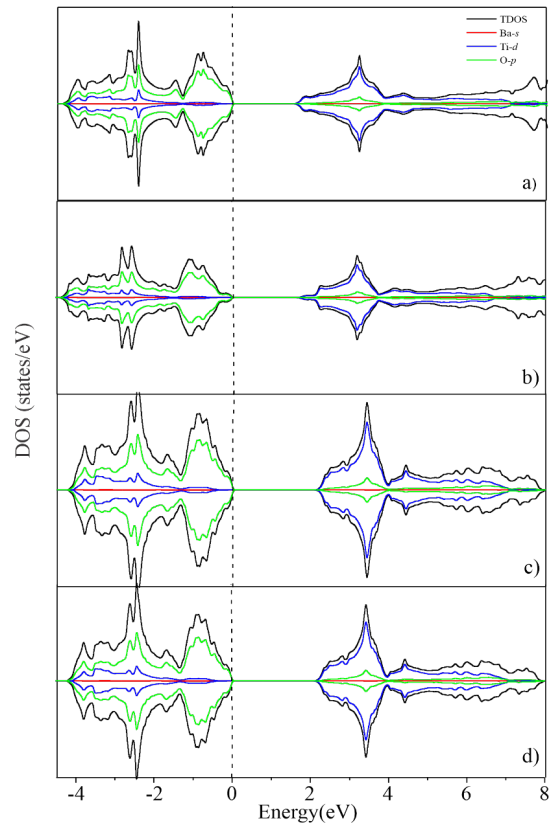|	Our results			Other theoretical data [7]		Experimental data	Ref.
	LDA	SCAN	PBE	LDA	PBE		
Cubic phase							
a, Å	3,95206	4,03462	4,03661	3,922	4,008	4,03558	[8]
bandgap $E_g (eV)$	1,08	1,09	1,08	1,93	1,87	3,2	[7]
Tetragonal phase							
a, Å	3,937	4,011	4,008	3,911	3,967	3,997	[8]
c, Å	4,031	4,157	4,188	3,967	4,232	4,0314	[8]
Δz_{Ti}	0,0203	0,0169	0,0182	0,0154	0,0335	0,0203	[8]
Δz_{O1}	-0,0258	-0,0392	-0,0409	–0,0210	–0,0431	-0,0258	[8]
Δz_{O2}	-0,0123	-0,0227	-0,0238	–0,0138	–0,0183	-0,0123	[8]
bandgap $E_g (eV)$	2	2,4	2	1,95	1,95	3,4	[7]
Orthorhombic phase							
a, Å	3,934	3,997	3,9954	3,911	3,955	3,9828	[8]
b, Å	5,6269	5,7843	5,7989	5,566	5,778	5,6745	[8]
c, Å	5,6411	5,8239	5,8397	5,576	5,836	5,6916	[8]
Δz_{Ti}	0,0122	0,0157	0,0158	0,0102	0,0253	0,0170	[8]
Δz_{O1}	-0,0140	-0,0197	-0,0205	–0,0109	–0,0173	-0,0110	[8]
Δy_{O2}	0,0043	0,0073	0,0071	–0,0010	– 0,0113	0,0061	[8]
Δz_{O2}	-0,0156	-0,0231	-0,0228	–0,0155	–0,0300	-0,0157	[8]
bandgap $E_g (eV)$	2,1	2,2	2,5	2,121	2,563	-	
Rhombohedral phase							
a, Å	3,9659	4,0702	4,0739	3,931	4,053	4,0036	[8]
α, deg	89,9039	89,7579	89,7568	89,92	89,65	89,840	[8]
Δx_{Ti}	-0,0099	-0,0143	-0,0138	–0,0073	–0,0190	-0,0120	[8]
Δx_O	0,0097	0,0142	0,0142	0,0101	0,0129	0,0116	[8]
Δz_O	0,0152	0,0244	0,0233	0,0144	0,0248	0,0195	[8]
bandgap $E_g (eV)$	2,2	2,2	2,5	2,234	2,796	-	

Figure 2. GGA density of states for the phase *BaTiO₃* (a) cubic, (b) tetragonal, (c) orthorhombic, (d) rhombohedral
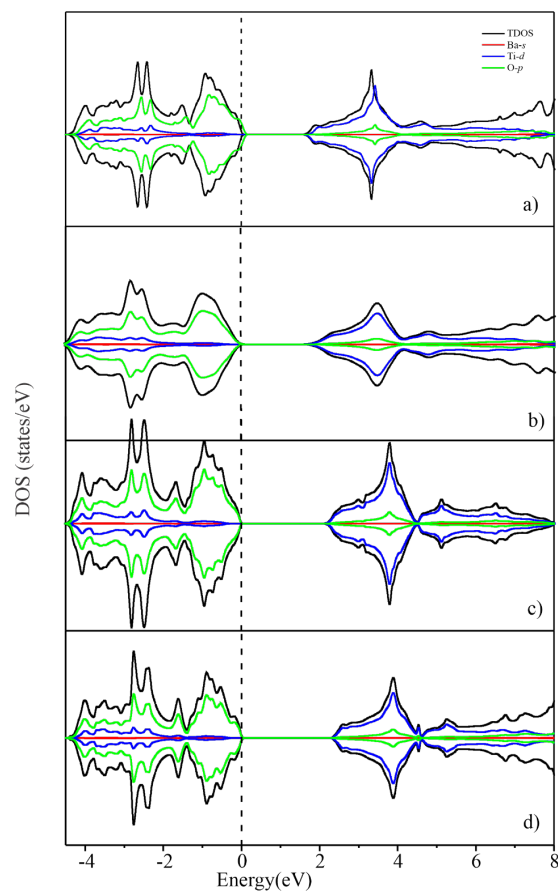

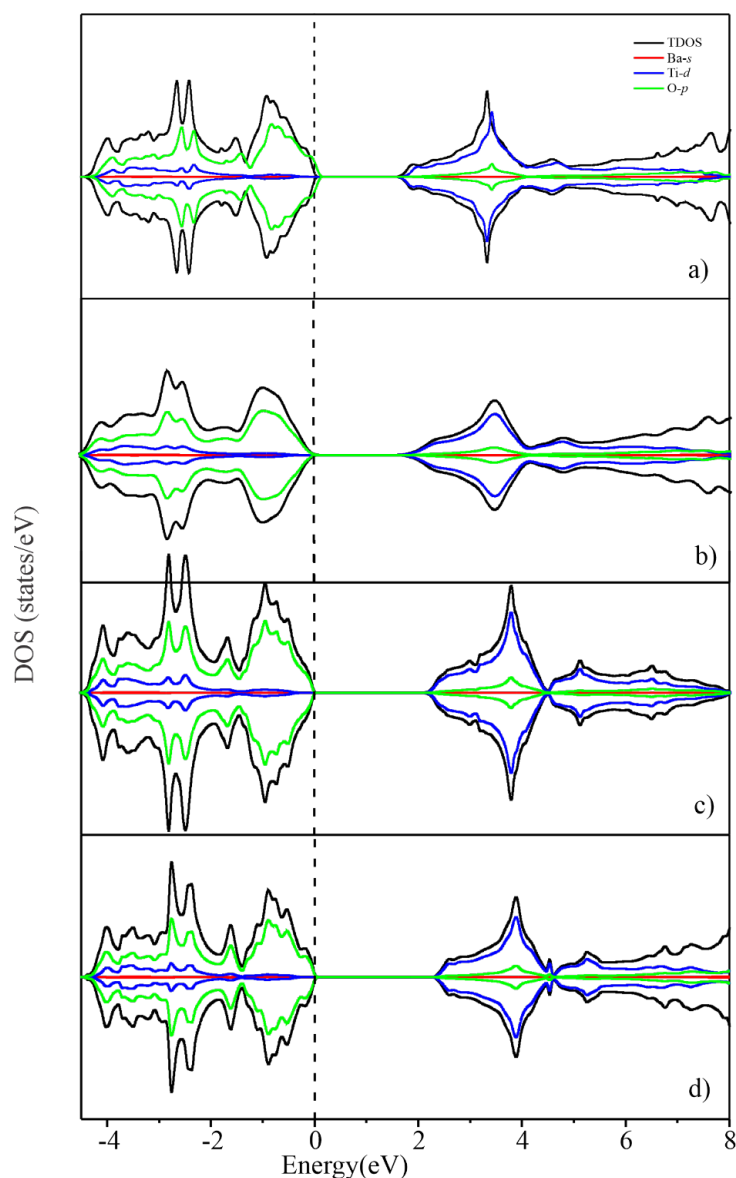Figure 3. SCAN density of states for the phase *BaTiO₃* (a) cubic, (b) tetragonal, (c) orthorhombic, (d) rhombohedral

Figure 4. LDA density of states for the (a) cubic, (b) tetragonal, (c) orthorhombic, (d) rhombohedral phase of *BaTiO₃*

Based on the first-principle calculations, the calculation of the BTO was carried out using the GGA - PBE, LDA, SCAN functionality for four modification of the perovskite structure. The obtained calculated values were compared with the experimental results. The lattice parameters *a, b, c* and the band gap are given in Table 2, the sequence of the arrangement of atoms are given in Table 1. For the rhombohedral phase, the angle of the lattice a is also shown. As can be seen from Table 2, the calculation using the PBE functional makes it possible to more accurately predict the cubic properties of BTO compared to other functionals [7]. When calculating with the PBE functional, one can see the correspondence between the experimental results' values of the lattice constant. The three ferroelectric phases of the BTO, as shown in the theoretical work [7], are calculated by the same DFT method. In these works, the structural properties of ferroelectric phases are considered. Table 2 shows a comparison of the results obtained with other theoretical values calculated with different functionals [7] and using experimental data for the crystals under study. LDA calculations [7] coincide with experimental data for BTO. On the other hand, as expected, the LDA and PBE functions significantly underestimate the band gap width. It can be seen that all DFT calculations do not estimate the band gap width, as shown in Figure 2. One of the shortcomings of the density functional theory method is inaccurate prediction of the free or excited state of semiconductor systems and dielectrics [10]. The calculated values by the SCAN functional do not differ much from the previous two functionals.

The band gap width is closely related to the difference in energy level between the valence band (VB) and the conduction band, which can be caused by structural distortions in the material.

Zone structures of the BTO using the functionals: PBE, LDA and SCAN for the four phases of BTO indicate that the energy of the band gap of the cubic structure is equal to: *Pm3m* 1.08 eV (LDA) and 1.09 eV (SCAN), 1.08 eV (PBE), tetragonal structure *P4/mmm* 2 *e*V (LDA) and 2.4 *e*V (SCAN), 2 *e*V (PBE), orthorhombic structure *Amm2* 2.1 *e*V (LDA) and 2.2 *e*V (SCAN), 2.5 *e*V (PBE), and rhombohedral structure *R3m* 2.2 *e*V (LDA) and 2.2 *e*V (SCAN), 2.5 *e*V (PBE). Analyses of band structures and density of states (DOS) using the PBE, LDA and SCAN functionals for the four phases of BTO showed that the values of the forbidden zones are underestimated. A general analysis of DOS projected onto atoms and orbitals is presented in Figures 2-4. An analysis of the density of DOS states shows that the upper part (valence band) mainly consists of O 2*p* orbitals. The lower part (conduction band) mainly comes from Ti 3*d* orbitals in all phases.

The conduction band for the tetragonal phase using the PBE, LDA and SCAN functionals consists of Ti 3*d* states, as well as the orthorhombic phase. The rhombohedral phase has a mixed composition of Ti states in the conduction band with a greater degree of $3d_{z2}$ than $3d_{xy}$. The projected state densities (PDOS) on atoms and orbitals are shown in Figure 2-4. The values of the band gap energy (E_{gap}) calculated using the PBE, LDA and SCAN functionals, as well as available theoretical and experimental data are shown in Table 2. The calculated values show reasonable agreement with previous theoretical results.

Conclusion

In this paper, the structure of stable phases is investigated using first-principle calculations based on the functionals: LDA, GGA- PBE and meta-GGA. When analyzing the electronic structures, the energies of the band gap were determined for the cubic structure: *Pm3m* 1.08 *e*V (LDA) and 1.09 *e*V (SCAN), 1.08 *e*V (PBE), for the tetragonal structure: *P4/mmm* 2 *e*V (LDA) and 2.4 *e*V (SCAN), 2 *e*V (PBE) for the orthorhombic structure: *Amm2* 2.1 *e*V (LDA) and 2.2 *e*V (SCAN), 2.5 *e*V (PBE) and for rhombohedral structure: *R3m* 2.2 *e*V (LDA) and 2.2 *e*V (SCAN), 2.5 *e*V (PBE). The data obtained for the density of states (DOS) showed that the upper part (valence band) mainly consists of O 2*p* orbitals, and the lower part (conduction band) comes from Ti 3*d* orbitals. The rhombohedral phase has a mixed composition of Ti states in the conduction band with a greater degree of $3d_{z2}$ than $3d_{xy}$. The values of the energies of the band gap (E_{gap}) and the density of states present reasonable agreement with experimental and theoretical data. The deviation in the theoretical calculations of the lattice parameters carried out in [7] using the LDA and PBE functionals in comparison with the results of the experimental study is 3 %. The deviation of calculations with our theoretical calculations using the LDA and PBE functionals was approximately the same as the authors [7], while the calculation with the Scan functional showed 0.02 % compared to the experimental result.

Acknowledgements

References

1   Steele, C.H., & Heinzel, A. (2001). Materials for fuel-cell technologies. *Nature, 414,* 345-352.

2   Abuova, A.U., Mastrikov, Y.A., & Kotomin, E.A. (2019). First-Principles Modeling of Oxygen Adsorption on Ag-Doped LaMnO₃ (001) Surface. *J. Electron. Mater, 49,* 1421–1434.

3   Abuova, A.U., Mastrikov, Yu.A., Kotomin, E.A., Kawazoe, Y., Inerbaev, T.M., & Akilbekov, A.T. (2015). First principles modeling of Ag adsorption on the LaMnO₃ (001) surfaces. *Solid State Ionics, 273, 46-50.*

4   Abuova, A.U., Akilbekov, A.T., Abuova, F.U., & Inerbaev, T.M. (2015). Modelling of structural and electronic properties surface (001) LaMnO₃ perovskite structure. *Condensed matter physics, 77,* 4-8.

5   Kuterbekov, K.A., Nurkenov, S.A., Rabotkin, S.V., Ionov, I.V., & Solovyev, A.A. (2021). Anode-supported solid oxide fuel cells with multilayer LSC/CGO/LSC cathode. *Fuel Cells, 21,* 408-412.

6   Woodward, P.M. (1997). Octahedral tilting in perovskites. II Structure stabilizing forces. *Acta crystallographica, 53,* 44.

7   Huai, Y.Z., Zhao, Y.Z., Ying, Q.Zh., Qing, L., & Yan, Ch. (2016). First-Principles Study of Lattice Dynamics, Structural Phase Transition, and Thermodynamic Properties of Barium Titanate. *Chemistry Physical,* 71, *759-768.*

8   Kwei, G.H., Lawson, A.C., Billinge, S.J.L., & Cbeong, S.W. (1993). Structures of the Ferroelectric Phases of Barium Titanate. *J. Phys. Chem.,* 97, 2368-2377.

9   Evarestov, R.A., & Bandura, A.V. (2012). First principles calculations on the four phases of BaTiO₃. *Journal of computational chemistry, 33,* 1123-1130.

10   Holm, B., Ahuja, R., Yourdshabyan, Y., Johanson, B., & Lundqvist, B.I. (1999). *Phys. Rev., 59,* 12777.

11 Sanna, S.C. (2011). Barium titanate ground and excited-state properties from first-principles calculations. *American Physical Society, 83,* 054112.

12 Kresse, G., & Furthmüller, J. (1996). Efficiency of ab-initio total energy calculations for metals and semiconductors using a plane-wave basis set. *Comput. Mater. Sci., 6,* 15-50.

13 Kresse, G., & Furthmüller, J. (1996). Efficient iterative schemes for ab initio total-energy calculations using a plane-wave basis set. *Phys. Rev., 54,* 11169.

14 Blöchl, P.E. (1994). Projector augmented−wave method. *Phys. Rev., 24,* 17953-17979.

15 Hohenberg, P., & Kohn, W. (1964). *Phys. Rev., 136,* 864.

16 Kohn, W., & Sham, L.J. (1965). *Phys. Rev., 140,* 1133.

17 Perdew, J.P., Burke, K., & Ernzerhof, M. (1996). *Phys.Rev., 77,* 3865-3868.

18 Sun, J., Remsing, R.C., Zhang, Y.Z., Sun, A., Ruzsinszky, H., Peng, Z., Yang, A., Paul, U., Waghmare, X., Wu, Klein, M.L., & Perdew, J.P. (2016). *Nat. Chem., 8,* 831-836.

19 Sun, J., Xiao, B., Fang, Y., Haunschild, R., Hao, P., Ruzsinszky, A., Csonka, G.I., Scuseria, G.E., & Perdew, J.P. (2013). *Phys. Rev., 111,* 106401.

20 Inerbaev, T.M., Matsuoka, T., & Kawazoe, Y. (2022). Optical band gap energy values in wurtzite In$_x$Ga$_{1-x}$N. *Bulletin of the university of Karaganda-Physics*, 105, *107-116.*

Т.М. Инербаев, Ж.Е. Зәкиева, Ф.У. Абуова, А.У. Абуова, С.А. Нуркенов, Г.А. Каптагай

BaTiO₃ бойынша DFT зерттеулері

Тұрақты фазалардың құрылымы функционалдық функцияларға негізделген алғашқыпринципті есептеулердің көмегімен зерттелген: LDA, GGA және жақында әзірленген әмбебап қатты шектелген және сәйкесінше нормаланған мета-GGA функционалы (SCAN). Бұл жұмыстың мақсаты тығыздық функционалы теориясы әдісін қолдана отырып, LDA, GGA-PBE және мета-GGA функционалдарын салыстыру үшін кубтық, тетрагональды, орторомбты, ромбоэдрлік перовскит фазаларының кристалдағы атом координаттарының өзгерісі мен рұқсат етілмеген аумақты теориялық тұрғыдан зерттеу. Алынған күйлердің тығыздығы (DOS) деректері тыйым салынған аймақта энергия мәнінің төмендегенін; ал DOS мәндерінің жоғарғы бөлігі (валенттік аумақ) негізінен O $2p$-орбитальдарынан, төменгі бөлігі (өткізгіштік аумақ) Ti $3d$ орбитальдарынан тұратынын көрсетті. Ромбоэдрлік фазада $3d_{xy}$-ге қарағанда $3d_{z2}$ үлкен дәрежелі өткізгіштік аумағында Ti күйлерінің аралас құрамы бар. Рұқсат етілмеген аумақ (E_{gap}) және күйлердің тығыздығы эксперименттік және теориялық мәліметтермен сәйкестігін көрседеді. LDA функционалдығы және аз дәрежеде GGA-PBE функционалдығы да осы кристалдардағы атомдық орын ауыстырулар туралы жеткілікті дәл ақпарат бере алады. SCAN функциясынан есептелген мәндер GGA және LDA функцияларынан аз ерекшеленеді.

Кілт сөздер: перовскит, қарапайым ұяшықтар, күйлердің тығыздығы, атомдардың ығысуы, тыйым салынған аймақ, алғашқыпринципті есептеулер, тығыздық функционалының теориясы, жазық толқындар, кеңістіктік топ.

Т.М. Инербаев, Ж.Е. Закиева, Ф.У. Абуова, А.У. Абуова, С.А. Нуркенов, Г.А. Каптагай

DFT исследования BaTiO₃

Структура стабильных фаз исследована с помощью первопринципных расчетов на основе функционалов: LDA, GGA и недавно разработанного универсального сильно ограниченного и соответствующим образом нормализованного мета-GGA-функционала (SCAN). Целью данной работы является теоретическое исследование атомных смещений и ширины запрещенной зоны кубической, тетрагональной, орторомбической, ромбоэдрической фаз перовскита для сравнения функционалов LDA, GGA-PBE и мета-GGA с использованием метода теории функционала плотности. Полученные данные плотности состояний (DOS) показали, что значения энергии запрещенной зоны занижены, а значения DOS указывают, что верхняя часть (валентная зона), в основном, состоит из O $2p$-орбиталей, нижняя часть (зона проводимости) — из $3d$-орбиталей Ti. Ромбоэдрическая фаза имеет смешанный состав состояний Ti в зоне проводимости с большей степенью $3d_{z2}$, чем $3d_{xy}$. Значения энергий запрещенной зоны (E_{gap}) и плотности состояний показывают разумное согласие с экспериментальными и теоретическими данными. Функционал LDA и, в меньшей степени, функционал GGA–PBE также могут дать достаточно точную информацию о смещениях атомов в этих кристаллах. Значения, рассчитанные по функционалу SCAN, мало чем отличаются от функционалов GGA и LDA.

Ключевые слова: перовскит, элементарная ячейка, плотность состояний, искажение атомов, запрещенная зона, первопринципные расчеты, теория функционала плотности, плоские волны, пространственная группа.